Journal of Applied Polymer Science

Novel Polyimide/Graphene Oxide Composite Films with Ultralow Dielectric Constants

Yang Zhi-Qiang,[1] Yuan Yuan,[1,2] Li Feng-Ling,[1] Liao Rui-Jin[2]

[1]College of Materials Science and Engineering, Chongqing University, Chongqing 400044, China

[2]State Key Laboratory of Power Transmission Equipment & System Security and New Technology, Chongqing University, Chongqing 400044, China

Correspondence to: Y. Yuan (E-mail: yuany@cqu.edu.cn)

ABSTRACT: Graphene is generally used for conductive material; it can also be used as a key nanofiller for the insulation material of inverter motors. In this study, a series of polyimide (PI) films were prepared successfully by a conventional two-step polymerization method based on bis[3,5-dimethyl-4-(4-aminophenoxy)phenyl]methane as a diamine and 4,4′-(hexafluoroisopropylidene)diphthalic anhydride as a dihydride with different weight percentage graphene oxide (GO) nanosheets as nanofillers. The dielectric constant (ε) and dielectric loss (tan δ) of these films were measured. The results show good dielectric properties, especially an ultralow ε value of 1.41 at 1 MHz with 0.19% GO. This showed that the low ε value was caused by a high free volume led by the GO nanosheets and the C—F bond. The structure and micromorphology of the PIs were characterized by X-ray diffraction and scanning electron microscopy. © 2014 Wiley Periodicals, Inc. J. Appl. Polym. Sci. **2015**, *132*, 41385.

KEYWORDS: dielectric properties; films; polyimides

Received 4 May 2014; accepted 8 August 2014

DOI: 10.1002/app.41385

INTRODUCTION

As high-performance polymers, polyimides (PIs) are widely used in optoelectronics, adhesives, and aerospace engineering and in the microelectronics industry because of their high electrical resistivity, high thermal stability, excellent mechanical properties, and chemical stability. In particular, PIs are important materials for the electrical industry because of their low dielectric properties.[1–4] Many studies have been done to explore low-dielectric-constant PIs in recent decades. It is well known that composing with inorganic/organic nanometer materials is an efficient approach that does not detrimentally affect the thermal and mechanical properties.[5] As a key part of the insulation in inverter motors, PI is directly related to operation reliability of an inverter motor. Nowadays, with the development of high impact voltages and insulation levels for inverter motors, the performance of PI films becomes one of the top issues, both in industrial and academic circles, especially with regard to the dielectric properties. However, PI films still cannot meet the development needs for inverter motors.

Previously, Tan et al.[6] developed a PI film with a dielectric constant (ε) of 2.1 by composing it with polyoxometalate. It was also reported in 2012 that ε was decreased to 1.9 via the addition of silica to fluorinated PIs.[7] In our previous work, PIs were achieved with bis[3,5-dimethyl-4-(4-aminophenoxy)phenyl]methane (BDAPM) as a diamine and different dihydridemonomers. The results show that PI–4,4′-(hexafluoroisopropylidene)diphthalic anhydride (6FDA) possessed the lowest ε of 2.6 at 1 MHz because of the low electronic polarizability of the C—F bond.[8] Then, various weight percentages of SiO_2 hollow spheres were added to PI–6FDA to gain novel PIs. Finally, ε was reduced to 1.8 with a 3% content.[4]

Graphene, first reported in 2004, for which the researchers won the 2010 Nobel Prize, has already attracted great interest.[9–11] It can be applied to the development of novel materials because of its special chemical structure, which conducts in plates but insulates between layers.[12] As a world famous conductor with outstanding characteristics, graphene displays enormous potential for high-performance electronic devices, mechanical materials, energy storage applications, and gas sensors.[13,14] All graphene-based materials, including graphene oxide (GO), graphene nanoplatelets, and graphene nanosheets, can make certain improvements to the properties of polymers. However, few researches have thus far reported the preparation of insulation materials with graphene. When used for the preparation of insulation materials, GO is the one of the best choices for further applications.[15–18]

In this study, PIs were successfully prepared on the basis of PI–6FDA and GO with different weight percentages in the range

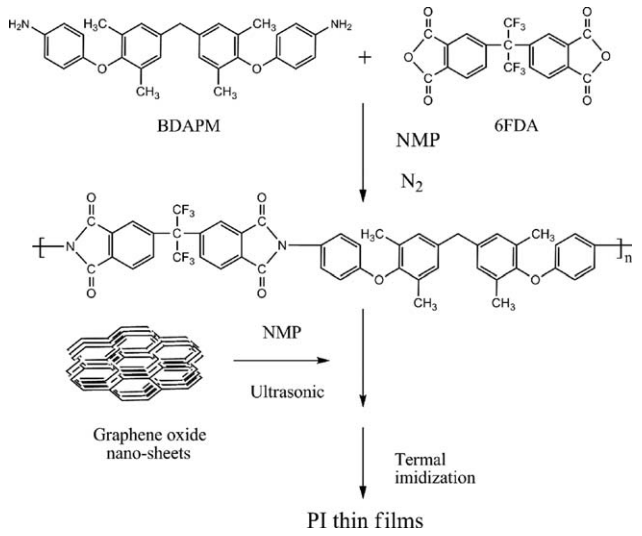

Figure 1. Preparation routes of the PI/GO composite films.

0–0.26%. Then, the dielectric properties, morphologies, structures, and so on of the PIs were investigated. The results show that the PIs composed of 0.19 wt % GO had significantly decreased ε values.

EXPERIMENTAL

Materials

6FDA was purchased from Sigma-Aldrich. Before use, it was recrystallized from acetic anhydride and dried *in vacuo*. Other chemical reagents in the experiments (all from Shanghai Chemical Reagents, Shanghai, China) were used as received, except for 1-methyl-2-pyrrolidinone (NMP) and *N*,*N*-dimethylformamide, which were purified by distillation *in vacuo* after being dried by P_2O_5.

Preparation of GO

GO was prepared from natural graphite powder according to a conventional Hummers' method.[19,20] Five grams (5 g) of graphite and 2.5 g of sodium nitrate were stirred with 115 mL of sulfuric acid (98%). Then, the mixture was cooled in an ice bath. An amount of 15 g of potassium permanganate was then added over a period of 2 h with vigorous stirring. In the subsequent 4 h, after the sample was heated to 35°C for 30 min, the reaction mixture was allowed to reach room temperature. The reaction mixture was then poured into a flask containing 250 mL of deionized water and further heated to 70°C. Before it was poured into 1 L of deionized water, the reaction mixture was held at a constant temperature for 15 min. With the addition of 3% hydrogen peroxide, the unreacted potassium permanganate and manganese dioxide were removed. Then, the reaction mixture was allowed to settle and decanted. The GO obtained was then purified by repeated centrifugation and redispersal in deionized water until a negative reaction on sulfate ion [with $Ba(NO_3)_2$] was achieved. The GO slurry was then dried in a vacuum oven at 60°C for 48 h before use.

Synthesis of BDAPM

First, bis[3,5-dimethyl-4-(4-nitrophenoxy)phenyl]methane (BDNPM) was synthesized according to a literature method.[19] In the presence of potassium carbonate (28.1 g, 0.2 mol) and *N*,*N*-dimethylformamide (300 mL), BDNPM was synthesized by the reaction of bis[3,5-dimethyl-4-phenol]methane (25.6 g, 0.1 mol) and *p*-chloronitrobenzene (31.5 g, 0.2 mol) at 150–160°C for 12 h. The solution was poured into distilled water after it was cooled to room temperature. A yellow powder was obtained by filtration and dried at 80°C. Then, 50 mL of hydrazine monohydrate was added dropwise to a mixture containing 25.9 g (0.052 mol) of BDNPM, 3.1 g (0.02 mol) of ferric chloride, 0.3 g of 5% Pd/C, and 200 mL of anhydrous ethanol at 70°C. The reaction was subsequently continued at 80–90°C for another 14 h. Finally, the product was filtered and recrystallized with anhydrous ethanol. After the purification, yellow crystals of BDAPM were prepared successfully.

Preparation of the PIs

As shown in Figure 1, the PIs were prepared by a conventional two-step polymerization method.[21] Typically, molar equivalents (0.001 mol) of BDAPM and 6FDA were added to dried NMP with a 10% solid concentration under a nitrogen atmosphere at room temperature for 24 h. Then, GO powder was added in NMP at different mass ratios and dispersed ultrasonically for 0.5 h. The mixture was dropped into the solution prepared previously and stirred for 6 h at room temperature; this was followed by ultrasonic dispersion for 0.5 h again. The solution was spread on a glass plate and placed in an 80°C vacuum oven for 2 h to remove the solvent. At last, the composite thin films were obtained after sequential heating from 80 to 240°C for about 7 h with the process of imidization. (As we all know, the density of GO was extremely low, and the general doping amount of GO may have led to unsuccessful preparation.)

Characterization

The ε and dielectric loss (tan δ) values were measured by a Novo Control broadband dielectric spectrometer with the films over various frequency from 1 Hz to 1 MHz at room temperature. Transmission electron microscopy (TEM) observations were conducted with a LIBRA 200 FE (Zeiss, Jena, Germany) at 120 kV. During testing, GO was spread on copper mesh with amorphous carbon films. The morphologies of the cross-sectional surface of the GO and PIs were observed on a NOVA400 field emission scanning electron microscope (FEI) with a working voltage of 10 kV. The composites were fractured first in liquid nitrogen and mounted on conductive glass by means of double-sided adhesive tape; then, a thin layer of gold was sputtered onto the cross-sectional surface before scanning electron microscopy (SEM) observation. The condensed structure was analyzed by X-ray diffraction (XRD) on a DMAX-1200 (Rigaku Corp., Tokyo, Japan) with 2θ changes from 5 to 45° at a scan speed of 4°C/min and with Cu Kα radiation ($\lambda = 0.154$ nm) as the X-ray source.

RESULTS AND DISCUSSION

The PI synthesized from BDAPM and 6FDA without GO was designated as PI–BDAPM–6FDA and that with 0.13 wt % GO was designated as PI–BDAPM–6FDA-0.13%. The rest were designated as PI–BDAPM–6FDA–0.19% and PI–BDAPM–6FDA-0.26%.

GO

Figure 2 shows the TEM images of GO. As shown in Figure 2(a), the lamellar structure of the GO nanosheets with few folds

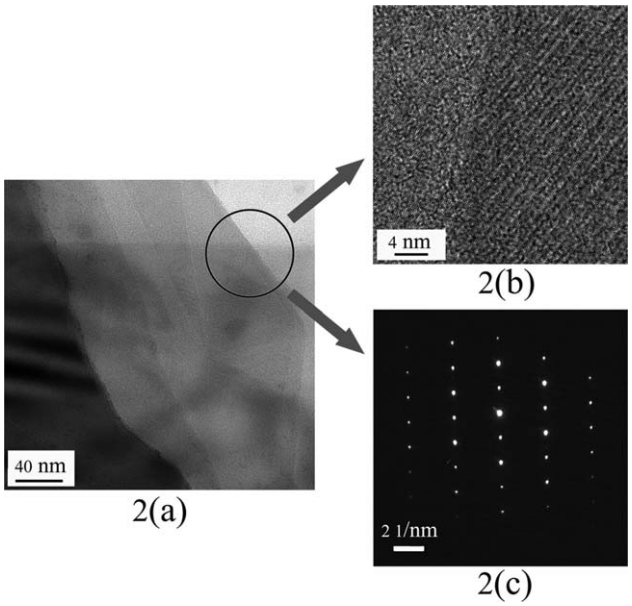

Figure 2. TEM images of GO.

were obvious. Meanwhile, a single layer shown in Figure 2(a) was chosen to obtain an HRTEM image. As shown in Figure 2(b), the amorphous carbon film was on the left side, whereas the other side represented graphene crystals. About 14 layers of GO were clearly observed. In Figure 2(c), the diffraction pattern of the field of GO is shown; this is a typical single crystal.

The structure of GO was investigated by XRD, and the spectrum is shown in Figure 3. This indicates the crystal structure of GO for the five characteristic peaks. An extremely strong peak appeared at $2\theta = 26.38°$ for the (002) plane; likewise, there were four weak peaks at $2\theta = 44.39$, 54.54, 77.24, and 83.18°; these corresponded to the GO (101), (004), (110), and (112) planes, respectively.

Dielectric Properties

As a representative of the ability to store charges, the ε value is a crucial parameter of the dielectric materials. Figure 4(a) shows

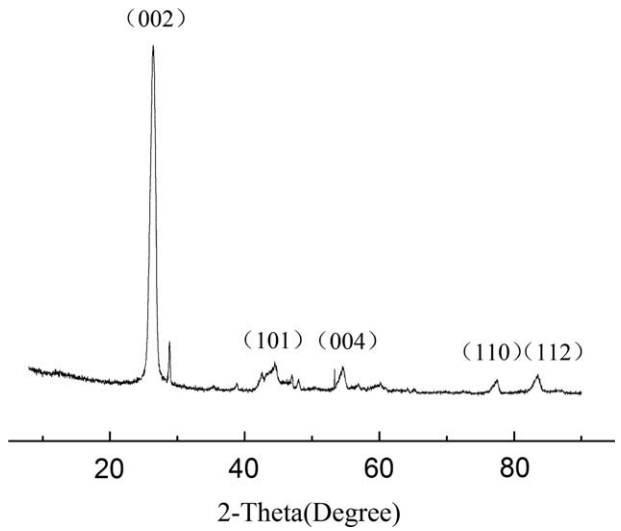

Figure 3. XRD spectrum of GO.

the relationships between the ε values and frequencies of PIs. It was obvious that the εs of PIs decreased slightly with increasing frequency; this resulted from the fact that the change in the dipole moment orientation could not catch up with the frequency of the electric field. The pure PI possessed the highest ε (only 2.17 at 1 MHz), and PI–BDAPM–6FDA-0.19% showed the lowest one, whereas the PI–BDAPM–6FDA-0.26% had the second lowest ε at the same frequency from 1 Hz to 1 MHz. As shown in Figure 4(b), the ε value of the PIs decreased from 2.17 to 1.41 and then increased to 1.70 at 1 MHz; however, the values were lower at 50 Hz. Compared with the results of other researchers, the pure PI in our study possessed a lower ε. It is well known that the use of fluorinated substituents into polymers can decrease ε because of the low electronic polarizability of the C—F bond and the increase in the free volume that accompanies the replacement of methyl groups by trifluoromethyl (CF_3) groups.[7,22,23] Meanwhile, the incorporation of free space caused by GO in the PI matrix effectively reduced ε of the composite.[24–27] Because the width of GO was 10s of micrometers in one direction, which was bigger than the thickness of the PI films, GO could only be parallel with the PI surface. The lamellar structure of GO tended to exclude close contact among

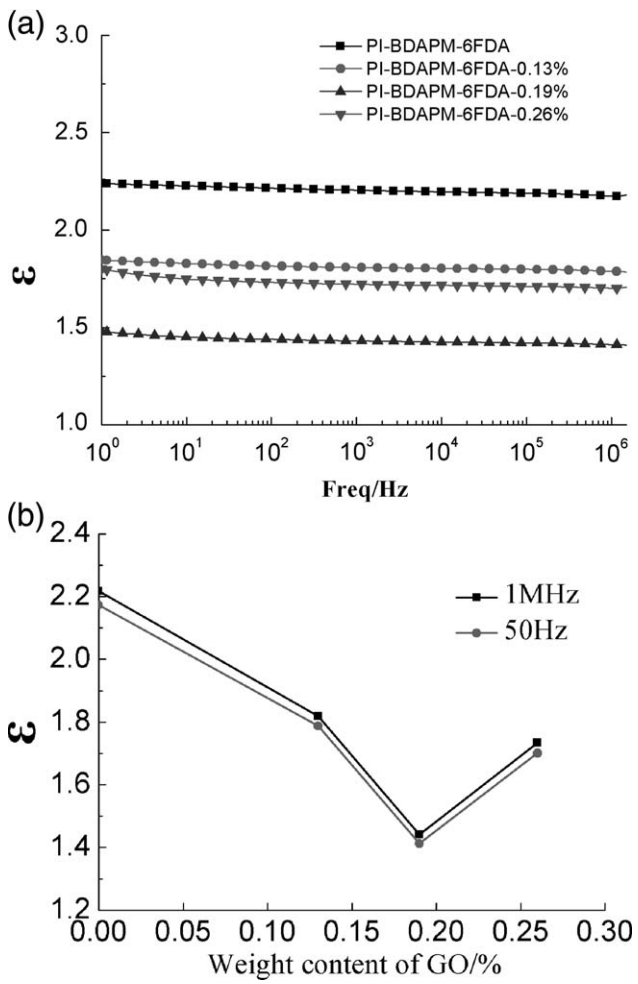

Figure 4. (a) Relationships between the ε values and frequencies of the four samples. (b) ε at 1 MHz and 50 Hz.

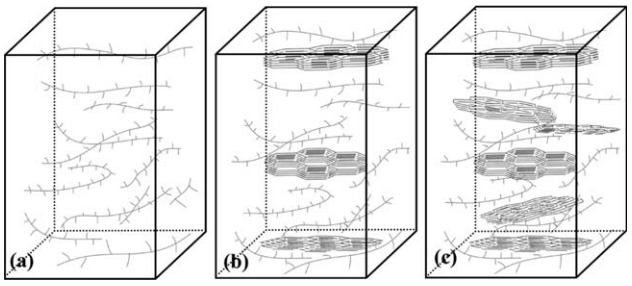

Figure 5. PIs (a) without GO, (b) with a certain amount of GO, and (c) with excessive GO.

the polymer matrix chains; this created a great free volume, as shown in Figure 5.[28,29] The ε value of air was 1.0, so the free volume in the PIs reduced the ε values of the whole composites.

When the amount of GO was in a small range, the ε values of PIs tended to be lower with increasing content of GO. The ε value fell with the addition of GO nanosheets. At the same time, what could not be ignored was that the strengthened interface between the PI matrix and GO within a composite led to a strong self-polarization-induced radical localization, which also decreased ε.[12] However, when the quality of GO was over 0.19 wt %, certain free volume would be occupied by excessive extra GO, and ε increased.

Tan δ, representing the energy loss, was also a vital parameter for insulation materials. Figure 6 shows the tan δ values of the PIs. At a frequency of 50 Hz, the pure PI expressed the lowest tan δ of 3.3790×10^{-3}, but PI–BDAPM–6FDA-0.26% possessed the highest value of 6.8035×10^{-3}. The curves of tan δ of the four samples performed the same trend of decreasing from a relatively high degree to an acceptable one lower than 0.01 with increasing frequency.

Morphology

The SEM images of the cross sections of the sample were used to evaluate the dispersion of GO in the polymer matrix. As shown in Figure 7(a), the GO sheets displayed a good dispersability on the fracture surface. During the process of ultrasonic dispersing, the GO was dispersed uniformly in the PI matrix.

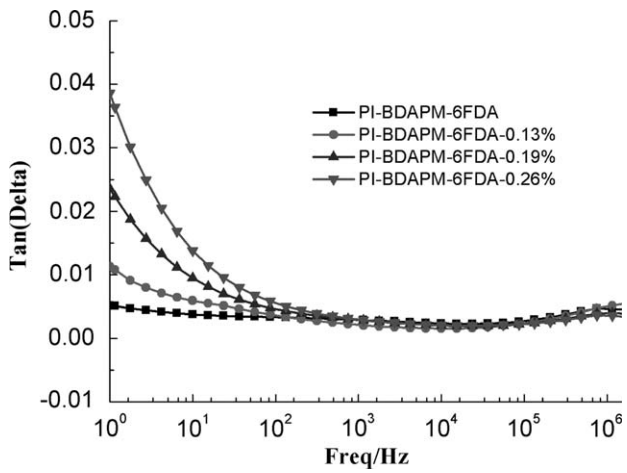

Figure 6. Tan δ values of the PIs.

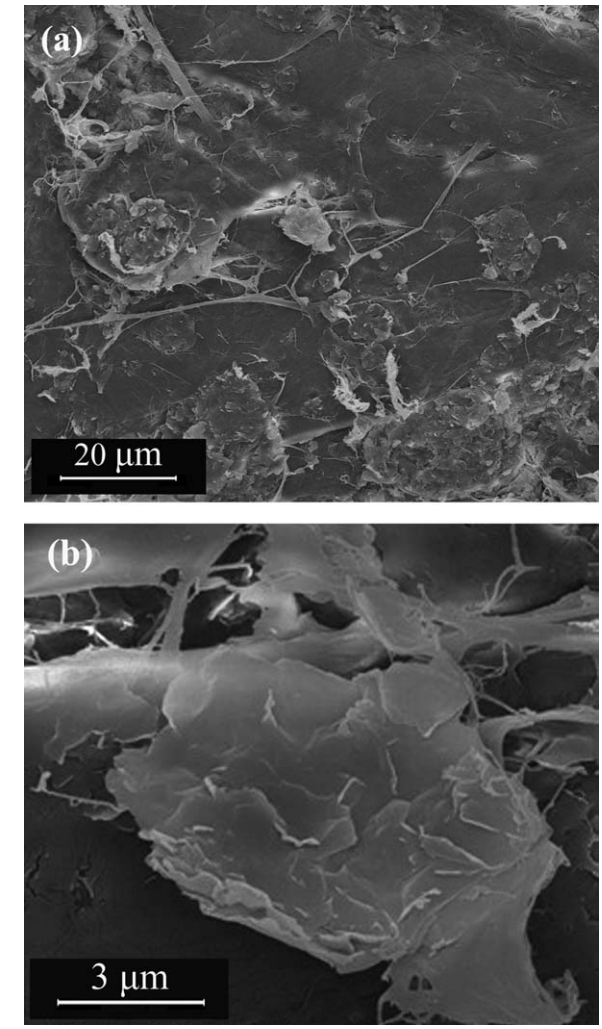

Figure 7. SEM images of the cross sections of the PI/GO films.

The lamellar structures of GO are shown more clearly in Figure 7(b). It was about several micrometers in one direction for one sheet in the center of this image. Furthermore, quite a bit of free volume existed between the GO and polymer matrix; this

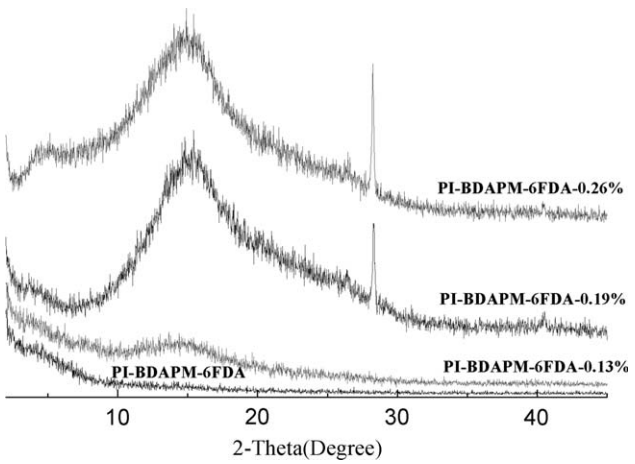

Figure 8. XRD spectra of the four samples.

led to a decrease in ε. Thus, it was an efficient approach to minimize the ε values of PIs via the incorporation of GO.

Structure

Figure 8 shows the XRD spectra of the PIs. It was obvious that there were no sharp diffraction peaks for pure PI. As for the PI/GO composite films, the strength of the characteristic diffraction peaks around about $2\theta = 28^\circ$ increased with the addition of GO. In contrast with pure PI, GO made a remarkable contribution to the structures of short-range order and even induced crystallization in a certain area as a result of the strengthening of the diffraction peak. When the XRD patterns of PI–BDAPM–6FDA-0.19% and PI–BDAPM–6FDA-0.26% were compared, the latter showed a stronger characteristic peak; this indicated more structures with a short-range order and the existence of less free volume. Consequently, PI–BDAPM–6FDA-0.19% possessed a lower ε.

CONCLUSIONS

A series of PIs with ultralow εs were prepared successfully by a conventional two-step polymerization method that was based on BDAPM as a diamine and 6FDA as a dihydride with the incorporation of GO sheets as an admixture. ε decreased to 1.41 at 1 MHz with a weight percentage of 0.19%; this was an extremely low value. It was ascribed to the effect of the free volume produced by the GO sheets as simulated in the study and was proven by the morphologies and structures of the samples.

ACKNOWLEDGMENTS

This work was supported by the Fundamental Research Funds for the Central Universities (project CDJZR 12130046), the Natural Science Foundation Project of ChongQing Chong Science and Technology Commission (CQ CSTC) (project cstcjjA50007), a special financial grant from the China Postdoctoral Science Foundation (contract grant number 2012T50763), a special financial grant from the Chongqing Postdoctoral Science Foundation (contract grant number XM20120037), and a general financial grant from the China Postdoctoral Science Foundation (contract grant number 2011M500142).

REFERENCES

1. Matsuura, T.; Hasuda, Y.; Nishi, S.; Yamada, N. *Macromolecules* **1991**, *24*, 500.
2. Chung, I.; Park, C. E.; Ree, M.; Kim, S. Y. *Chem. Mater.* **2001**, *13*, 2801.
3. Wang, J.-Y.; Yang, S.-Y.; Huang, Y.-L.; Tien, H.-W.; Chin, W.-K.; Ma, C.-C. M. *J. Mater. Chem.* **2011**, *21*, 13569.
4. Yuan, Y.; Lin, B.-P.; Sun, Y.-M. *J. Appl. Polym. Sci.* **2011**, *120*, 1133.
5. Chen, W. Y.; Ko, S. H.; Hsieh, T. H. *Macromol. Rapid Commun.* **2006**, *27*, 452.
6. Tan, L.; Liu, S.; Zeng, F.; Zhang, S.; Zhao, J.; Yu, Y.-E. *Polym. Adv. Technol.* **2009**, *22*, 209.
7. Zhang, Y. H.; Yu, L.; Su, Q.; Zheng, H.; Huang, H.; Chan, H. L. W. *J. Mater. Sci.* **2012**, *47*, 1958.
8. Yuan, Y.; Lin, B. P.; Sun, Y. M. *J. Appl. Polym. Sci.* **2007**, *104*, 1265.
9. Novoselov, K. S.; Geim, A. K.; Morozov, S. V. *Science* **2004**, *306*, 666.
10. Novoselov, K. S. *Rev. Mod. Phys.* **2011**, *83*, 837.
11. Eda, G.; Fanchini, G.; Chhowalla, M. *Nat. Nanotechnol.* **2008**, *3*, 270.
12. Dreyer, D. R.; Park, S.; Bielawski, C. W.; Ruoff, R. S. *Chem. Soc. Rev.* **2010**, *39*, 228.
13. Ren, P.-G.; Yan, D.-X.; Chen, T.; Zeng, B.-Q.; Li, Z.-M. *J. Appl. Polym. Sci.* **2011**, *121*, 3167.
14. Wang, J.; Hu, H.; Wang, X.; Xu, C.; Zhang, M.; Shang, X. *J. Appl. Polym. Sci.* **2011**, *122*, 1866.
15. Kim, H.; Abdala, A. A.; Macosko, C. W. *Macromolecules* **2010**, *43*, 6515.
16. Verdejo, R.; Bernal, M. M.; Romasanta, L. J.; Lopez Manchado, M. A. *J. Mater. Chem.* **2011**, *21*, 3301.
17. Dreyer, D. R.; Park, S.; Bielawski, C. W.; Ruoff, R. S. *Chem. Soc. Rev.* **2010**, *39*, 228.
18. Compton, O. C.; Nguyen, S. B. T. *Small* **2010**, *6*, 711.
19. Hummers, W. S.; Offeman, R. E. *J. Am. Chem. Soc.* **1958**, *80*, 1339.
20. Poh, H. L.; Sanek, F.; Ambrosi, A.; Zhao, G. J.; Sofer, Z.; Pumera, M. *Nanoscale* **2012**, *4*, 11.
21. Xing, Y.; Wang, D.; Gao, H.; Jiang, Z. *J. Appl. Polym. Sci.* **2011**, *122*, 738.
22. Jiang, L. Y.; Leu, C. M.; Wei, K. H. *Adv. Mater.* **2002**, *14*, 426.
23. Maex, K.; Baklanov, M. R.; Shamiryan, D. *J. Appl. Phys.* **2003**, *93*, 8793.
24. Vo, H. T.; Shi, F. G. *Microelectron. J.* **2002**, *33*, 409.
25. Tseng, M. C.; Liu, Y. L. *Polymer* **2010**, *51*, 5567.
26. Dang, Z. M.; Ma, L. J.; Zha, J. W.; Yao, S. H.; Xie, D.; Chen, Q.; Duan, X. *J. Appl. Phys.* **2009**, *105*, 044104.
27. Zha, J. W.; Jia, H. J.; Wang, H. Y.; Dang, Z. M. *J. Phys. Chem. C* **2012**, *116*, 23676.
28. Liu, Y. L.; Tseng, M. C.; Fanchiang, M. H. *J. Polym. Sci. Part A: Polym. Chem.* **2008**, *46*, 5157.
29. Liu, Y. L.; Fanchiang, M. H. *J. Mater. Chem.* **2009**, *19*, 3643.